Agricultural and Forest Meteorology xxx (2011) xxx–xxx

Contents lists available at ScienceDirect

Agricultural and Forest Meteorology

journal homepage: www.elsevier.com/locate/agrformet

Modeling water availability for trees in tropical forests

Fabien Wagner[a,*], Bruno Hérault[a], Clément Stahl[b], Damien Bonal[c], Vivien Rossi[d]

[a] Université des Antilles et de la Guyane, UMR 'Ecologie des Forêts de Guyane' BP 709, 97387 Kourou Cedex, France
[b] INRA, UMR 'Ecologie des Forêts de Guyane', 97379 Kourou Cedex, France
[c] INRA, UMR INRA-UHP 1137 'Ecologie et Ecophysiologie Forestière', 54280 Champenoux, France
[d] CIRAD, UMR 'Ecologie des Forêts de Guyane', 97379 Kourou Cedex, France

ARTICLE INFO

Article history:
Received 5 November 2010
Received in revised form 12 April 2011
Accepted 18 April 2011

Keywords:
Water balance model
Amazonian rainforest
Time domain reflectometer
Bayesian inference
Tree drought stress

ABSTRACT

Modeling soil water availability for tropical trees is a prerequisite to predicting the future impact of climate change on tropical forests. In this paper we develop a discrete-time deterministic water balance model adapted to tropical rainforest climates, and we validate it on a large dataset that includes micro-meteorological and soil parameters along a topographic gradient in a lowland forest of French Guiana. The model computes daily water fluxes (rainfall interception, drainage, tree transpiration and soil plus understorey evapotranspiration) and soil water content using three input variables: daily precipitation, potential evapotranspiration and solar radiation. A novel statistical approach is employed that uses Time Domain Reflectometer (TDR) soil moisture data to estimate water content at permanent wilting point and at field capacity, and root distribution. Inaccuracy of the TDR probes and other sources of uncertainty are taken into account by model calibration through a Bayesian framework. Model daily output includes relative extractable water, *REW*, i.e. the daily available water standardized by potential available water. The model succeeds in capturing temporal variations in *REW* regardless of topographic context. The low Root Mean Square Error of Predictions suggests that the model captures the most important drivers of soil water dynamics, i.e. water refilling and root water extraction. Our model thus provides a useful tool to explore the response of tropical forests to climate scenarios of changing rainfall regime and intensity.

1. Introduction

Despite annual precipitation that always exceeds 1500 mm year^{-1}, most of the Amazon's neotropical forests experience some annual dry season (less than 100 mm per month), that is variable in both duration and intensity (Malhi and Wright, 2004; Sombroek, 2001; Xiao et al., 2006; Marengo, 1992).

The consequences of annual drought on tropical forest functioning include a decrease in growth primary production and ecosystem respiration (Goulden et al., 2004; Hutyra et al., 2007; Bonal et al., 2008), and a reduction in tropical tree fluxes for both carbon (Bonal et al., 2000; Miranda et al., 2005) and water fluxes (Fisher et al., 2006). Very recently, an analysis of tree responses to the intense 2005 dry season highlighted the vulnerability of neotropical forests to moisture stress, with the potential for positive feedbacks on climate change due to increased tree mortality (Phillips et al., 2009).

Climate modeling scenarios suggest that the dry season in north-eastern Amazonian forests might lengthen during the 21st century (Cox et al., 2000, 2004; Malhi and Wright, 2004; Malhi et al., 2009). The short-term effect of soil water availability deficits on tropical tree growth, mortality and carbon and water fluxes has recently been quantified under experimentally controlled conditions (Fisher et al., 2007; Nepstad et al., 2007). Long-term inventory plots with regular tree censuses (growth, recruitment, mortality) have been set-up widely in the past few decades throughout Amazonia (Phillips et al., 2010; Clark, 2004; Wagner et al., 2010). These plots offer an unexpected opportunity to analyze the impact of soil water availability on tropical forest dynamics on a large temporal and spatial scale (Clark, 2007). However, to the best of our knowledge, no soil water balance model explicitly accounting for tropical soil and climate characteristics, and able to compute available water for the trees on a plot scale, has ever been developed. The relation between amount of rainfall and water availability for trees is not straightforward and determined by various plant characteristics, such as the root distribution, and soil characteristics, such as the permanent wilting point and the field capacity. By contrast, other widely studied climatic variables such as light and temperature give a relatively direct indication on their effect on forest dynamics (Graham et al., 2003; Clark et al., 2010). Soil water availability to the trees, which can be characterized by Relative Extractable Water (*REW*, i.e. daily available water standardized by maximum available water), depends on soil characteristics such as structure, texture, composition and porosity, as well as on the rate of water uptake by the trees. Different soil water balance models

* Corresponding author. Tel.: +594 594329217.
E-mail address: fabien.wagner@ecofog.gf (F. Wagner).

0168-1923/$ – see front matter © 2011 Elsevier B.V. All rights reserved.
doi:10.1016/j.agrformet.2011.04.012

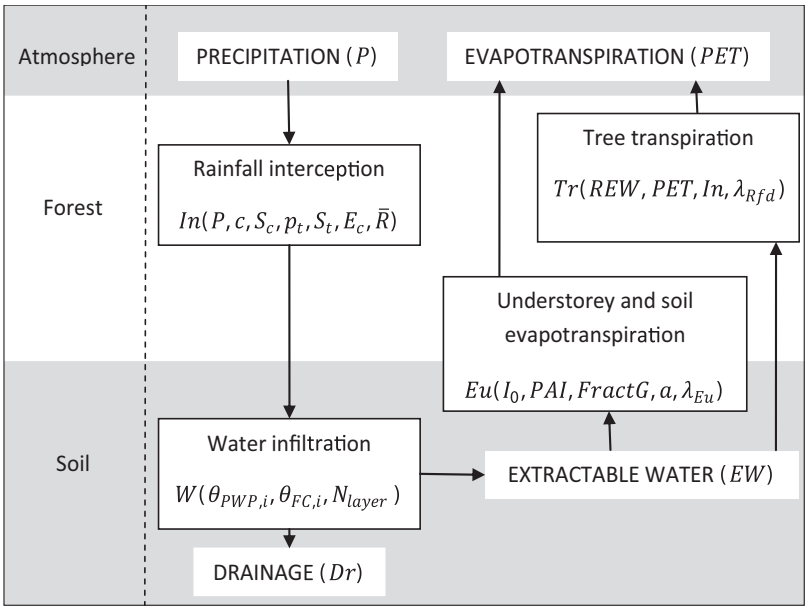

Fig. 1. Overview of the Soil Water Balance model general framework and the articulation of the different submodels, P: precipitation, c: canopy cover, S_c: canopy capacity, p_t: proportion of rain diverted to the trunks, S_t: trunk capacity, E_c: mean evaporation rate from the canopy, $\bar{R}$: mean rainfall rate, θ_{PWP}: soil water content at permanent wilting point, θ_{FC}: soil water content at field capacity, N_{layer}: number of layers of the model, I_0 = net radiation, PAI: plant area index, $FractG$: reflected radiation below trees, a: constant of proportionality between energy and evapotranspiration of the understorey, λ_{Eu}: understorey root density parameter, REW: relative extractable water, PET: potential evapotranspiration, λ_{Rfd}: tree root density parameter.

have been used in Amazonian tropical forests to estimate drought implications for forest flammability and tree growth (Nepstad et al., 2004), to reproduce hydrologic processes (Belk et al., 2007), to evaluate soil water controls on evapotranspiration (Fisher et al., 2007), or to evaluate the importance of deep root uptake (Markewitz et al., 2010). However, none of these models aims to estimate *REW*. The nearest estimate of *REW* is so-called plant available water (*PAW*) described by Nepstad et al. (2004). The spatial resolution of *PAW*, i.e. 8 km, is too large for use in any precise modeling of the impact of soil drought conditions on tree growth, mortality and/or recruitment. Furthermore, the modeling framework never explicitly simulates the amount of water taken up by tree roots. Modeling approaches designed to estimate *REW* have already been developed for temperate forests and, for instance, were used to assess soil water control on carbon and water dynamics in European forests during the 2003 drought (Granier et al., 2007). Such temperate models are not suitable for tropical forests. For instance, the polynomial rainfall interception submodel is unsuited to the stand characteristics of tropical forests. Another limit is that water extraction is not modeled and field data is needed for root density, meaning that soil pits need to be dug to quantify vertical root distribution, also meaning that the strong assumption must be made that water absorption by roots is proportional to root distribution.

In this paper we introduce a locally parameterized soil water budget model inspired by the BILJOU temperate model (Granier et al., 1999). As performed by BILJOU, this model estimates soil water availability, stand transpiration and rainfall interception in tropical forests with a daily time step and for different soil types (Fig. 1). Model inputs are daily rainfall, annual means of potential evapotranspiration (*PET*) and solar radiation, and averaged plant area index (*PAI*). The soil is filled by rainfall water passing through the canopy. The amount of rainfall intercepted by the canopy is computed in a submodel adapted to tropical forests (Gash et al., 1995). In our model, the soil consists of a succession of fine layers, each of which has a unique field capacity and permanent wilting point. We developed a new method using a Bayesian framework to estimate these two parameters using only Time Domain Reflectometer (TDR) measurements. When the water in a given layer exceeds water content at field capacity, drainage occurs and water fills the next layer, etc. Water extraction from soil layers is due to tree transpiration in addition to soil and understorey evapotranspiration. Soil evaporation and understorey transpiration are computed based on equations developed by Granier et al. (1999), and are assumed to be proportional to the energy reaching the understorey; tree transpiration is computed using potential evapotranspiration. Both understorey and tree transpiration are extracted in accordance with estimated root distribution.

This paper has three specific objectives: (i) to present our water balance model and to describe the different submodels it contains; (ii) to present an original statistical method used to estimate permanent wilting point, field capacity, and root distribution based on Time-Domain Reflectometer (TDR) data only; and (iii) to parameterize and validate the model using TDR data collected on a soil topographic gradient in Paracou, French Guiana.

2. List of symbols and abbreviations

P	precipitation
In	rainfall interception
Th	throughfall
Tr	tree transpiration
PET	potential evapotranspiration
ρ	ratio Tr/ETP
Eu	understorey and soil evapotranspiration
Dr	drainage in depth
$\theta_{PWP,l}$	soil water content at permanent wilting point for layer l
$\theta_{FC,l}$	soil water content at field capacity of soil layer l
λ_{Rfd}	root density parameter
EW_l	extractable water of soil layer l
$EW_l^{\max}$	maximum extractable water of soil layer l, $\theta_{FC,l} - \theta_{PWP,l}$
REW	relative extractable water of the soil
$REWc_l$	REW of soil layer l, critical when ≤ 0.4

Please cite this article in press as: Wagner, F., et al., Modeling water availability for trees in tropical forests. Agric. Forest Meteorol. (2011), doi:10.1016/j.agrformet.2011.04.012

Table 1
Interception model components adapted from Cuartas et al. (2007).

Components of interception loss	Formulation of components
For a storm insufficient to saturate the canopy	cP_G
Wetting up the canopy for a storm $>P'_G$ which saturates the canopy	$cP'_G - cS_c$
Evaporation from saturation until rainfall ceases	$\frac{c\bar{E}_c}{\bar{R}}(P_G - P'_G)$
Evaporation after rainfall ceases	cS_c
Evaporation from trunks for a storm which saturates the trunk, $P_G > St/pt$	S_t
Evaporation from trunks for a storm insufficient to saturate the trunk	$p_t P_G$

3. The model

Our daily water balance model was constructed using discrete-time deterministic formalism. The model contains and interconnects four submodels that compute interception, water infiltration and deep drainage, tree transpiration, and soil plus understorey evapotranspiration (Fig. 1). First, part of the precipitation is intercepted by the canopy, then the remaining part reaches the soil surface and fills the soil. If the soil is at field capacity, the excess water is lost by deep drainage. Tree transpiration is assumed to absorb water from the soil depending on root distribution, and soil plus understorey evapotranspiration are assumed to absorb water from the top 1 m of soil. The daily change in soil water content is computed as:

$$\Delta EW = P - In - Tr - Eu - Dr \quad (1)$$

where ΔEW is the daily change in soil water content, P is the precipitation, In is the rainfall interception by the forest canopy, Tr is tree transpiration, Eu is evapotranspiration from soil plus understorey and Dr is drainage. We used Granier's framework for the general structure of the model (Granier et al., 1999, 2007).

3.1. Rainfall interception model

In tropical forests, rainfall interception by the forest canopy and the evaporation of intercepted rainfall constitute an important part of the ecosystem's water flux. The most commonly applied models are the original and sparse Rutter models (Rutter et al., 1971; Valente et al., 1997) and the original and sparse Gash model (Muzylo et al., 2009; Gash, 1979; Gash et al., 1995). The Gash model has been validated for tropical rainforests (Lloyd et al., 1988; Germer et al., 2006; Cuartas et al., 2007), and we estimate the daily rainfall interception using this model with a daily step, assuming one rainfall per day. To estimate In we need to determine canopy cover c, canopy capacity per unit area of cover S_c, the proportion of rain diverted to the trunks p_t, the trunk capacity S_t and the amount of rainfall needed to saturate the canopy P'_G given by:

$$P'_G = \frac{-\bar{R}S_c}{\bar{E}_c}\ln\left[1 - \frac{\bar{E}_c}{\bar{R}}\right] \quad (2)$$

where $\bar{R}$ is the mean rainfall rate for saturated canopy conditions and $\bar{E}_c$ is the mean evaporation rate from the canopy.

In our model we compute In under the assumption of one rainfall per day, and interception is computed as the sum of the components listed in Table 1.

3.2. Soil characteristics and drainage

The water reaching the soil (Throughfall, Th) for each day d is computed as:

$$Th_d = P_d - In_d \quad (3)$$

where P_d and In_d are precipitation and intercepted precipitation by the canopy, respectively, for day d.

The modeling of water dynamics in soil follows a layered bucket model frame. Soil is assimilated as a succession of 1 cm layers. Each layer has a field capacity and a permanent wilting point. For layer l, the difference between field capacity ($\theta_{FC,l}$) and permanent wilting point ($\theta_{PWP,l}$) is the maximum extractable water by the plant ($EW_l^{\max} = \theta_{FC,l} - \theta_{PWP,l}$). The extractable water in layer l for each day d is noted as $\widehat{EW}_{l,d}$.

When precipitation reaches the soil surface, the first layer is filled to field capacity before draining and filling the next layer to field capacity, continuing until no water remains. The model does not take account of surface runoff. If there is more water than total field capacity, the excess water is lost by deep drainage. Details of the algorithm are given in Appendix A.

A critical value is computed daily for each layer, i.e. critical relative extractable water $REWc$:

$$REWc_{l,d} = \frac{\widehat{EW}_{l,d} - \theta_{PWP,l}}{\theta_{FC,l} - \theta_{PWP,l}} \quad (4)$$

where $\theta_{PWP,l}$ and $\theta_{FC,l}$ are the permanent wilting point and the field capacity of layer l.

3.3. Understorey and soil evapotranspiration

The evapotranspiration of understorey and soil (Eu) is computed by assuming that it is proportional to the energy reaching this level (Granier et al., 1999). Available energy under the canopy is computed using the Beer Lambert equation, the extinction coefficient (k), plant area index (PAI) and net radiation (I_0), Eq. (5). Part of this energy is reflected ($FractG$) while the energy that remains is assumed to be proportional to understorey and soil evapotranspiration, applying coefficient a. We assume Eu to absorb water in the top meter of soil with an exponential function of parameter 0.5. For layer l, Eu_l is computed as:

$$Eu_l = I_0 \times \exp(-k \times PAI) \times (1 - FractG) \times a \times 0.5 \times \exp(-0.5 \times N_{layer,l}) \quad (5)$$

3.4. Tree transpiration

Tree transpiration is computed based on potential evapotranspiration (PET). Granier et al. (1999) observed, for a LAI greater than 6 and when the soil water content was unlimited (Relative Extractable Water, $REW > 0.4$), a constant ratio between tree transpiration and PET for temperate and tropical forest stands. When soil water content became limiting for plants ($REW < 0.4$), the ratio $\rho = Tr/PET$, decreased linearly (Granier et al., 1999). We made the assumption that under stress conditions ($REW < 0.4$), the ratio ρ decreases linearly to reach 0 when no water is available for the trees, Eq. (8). Tree transpiration is extracted from each layer in relation to root density. As the relationship between amount of roots and rooting depth follows an exponential function (Humbel, 1978), we used an exponential function to model fine root density (Rfd). Rfd is defined by:

$$Rfd(depth) = \lambda_{Rfd} \times \exp(-\lambda_{Rfd} \times depth) \quad (6)$$

Please cite this article in press as: Wagner, F., et al., Modeling water availability for trees in tropical forests. Agric. Forest Meteorol. (2011), doi:10.1016/j.agrformet.2011.04.012

where λ_{Rfd} is the root density parameter. The percentage of transpiration extracted between soil surface and layer l is the integral of Rfd between 0 and $depth_l$, the depth of layer l in cm. To simplify notation, we set Rfd_l as the percentage of transpiration extracted from layer l, which is defined by

$$Rfd_l = \int_{depth_{l-1}}^{depth_l} Rfd(depth)\mathrm{d}\,depth$$

Tree transpiration extracted for layer l and for day d is computed as:

$$Tr_{l,d} = \rho_l \times PET \times (1 - \exp(-\lambda_{Rfd} \times N_{layer})) \times Rfd_l \quad (7)$$

where

$$\rho_l = \begin{cases} \rho \quad if \quad REWc_{l,d} > 0.4 \\ (REWc_{l,d} \times \rho)/0.4 \quad \text{if} \quad REWc_{l,d} < 0.4 \end{cases} \quad (8)$$

3.5. Model output

The model outputs *REW* (Relative Extractable Water), a daily value between 0 and 1, is computed as follows:

$$REW_d = \sum_{l=1}^{N_{layer}} \frac{\widehat{EW}_{l,d} - \theta_{PWP,l}}{\theta_{FC,l} - \theta_{PWP,l}} \times \frac{Rfd_l}{\sum_{l=1}^{N_{layer}} Rfd_l} \quad (9)$$

REW is computed from the soil surface to the depth of the N_{layer}. When $REW = 1$, the amount of extractable water by the tree is at its maximum and, when $REW = 0$, no water is available for trees. A *REW* of less than 0.4 is considered to represent hydric stress for temperate and tropical forest trees (Granier et al., 1999; Stahl and Bonal, unpublished data). This *REW* is weighted by root density (*Rfd*) in order to limit the weight of layers that are full of extractable water but contain few or no roots.

4. Calibrating and testing the model

4.1. Site descriptions and experimental setup

The study site used for calibration is located in Paracou, French Guiana (5°18′N, 52°55′W), a lowland tropical rain forest near Sinnamary (Gourlet-Fleury et al., 2004). The forest is typical of Guianan rainforests (ter Steege et al., 2006). More than 550 woody species attaining 2 cm DBH (Diameter at Breast Height) have been described at the site, with an estimated 160–180 species of trees ≥10 cm DBH per hectare. The dominant families at the site include Leguminoseae, Chrysobalanaceae, Lecythidaceae, Sapotaceae and Burseraceae. The climate is affected by the north/south movements of the Inter-Tropical Convergence Zone and the site receives nearly two-thirds of its annual 3041 mm of precipitation between mid-March and mid-June, and less than 50 mm per month in September and October. The site is located approximately 40 m above sea level (Gourlet-Fleury et al., 2004) and is made up of a succession of small hills with slopes of less than 30% (Ferment et al., 2001; Ferry et al., 2010).

In 2003, a 55 m self-supporting metallic eddy covariance flux tower, Guyaflux, was built in the Paracou forest in a natural 100 m^2 gap, with minimal disturbance to the upper canopy. This location covers a range of more than 1 km of forest in the direction of the prevailing winds. The top of the tower is about 20 m higher than the overall canopy and meteorological and eddy flux sensors are mounted 3 m above the tower. Full details on tower sensors are given by Bonal et al. (2008). Potential evapotranspiration (*PET* in mm), was computed based on the Penman–Monteith equation (Allen et al., 1998) from meteorological data gathered by tower sensors.

Soils were mapped based on a soil classification developed in French Guiana (Boulet et al., 1993; Sabatier et al., 1997) which defines seven functional units corresponding to seven successive evolutionary stages in a ferralitic soil. The first stages involve the thinning of a miggroaggregated upper horizon, whereas the second stages describe the mineralogical changes that occur under different hydromorphic conditions. The evolutionary degree of the ferralic cover is also related to the soil's hydrodynamic functioning and chemical properties (Sabatier et al., 1997). The seven functional soil units are referred to as DVD (deep vertical drainage), Alt (red alloterite at a depth of less than 1.2 m), SLD (superficial lateral drainage), UhS (uphill system), UhS+DC (uphill system + dry character, i.e. horizons at a depth of less than 1 m are *dry to the touch* in all seasons), DhS (downhill system) and DhS+DC (Downhill system + dry character). Humbel (1978) observed similar patterns of vertical root distribution within soils with vertical drainage (Alt, Uhs, DVL), or superficial lateral drainage (SLD). Root distribution is very extensive in the upper horizon with more than 80% of the fine roots found in the top 60 cm. The presence of fine roots decreases exponentially with depth. Rooting depth has not been investigated at our study site but potentially extends to 10 m, as observed elsewhere in the Amazon basin (Markewitz et al., 2010).

Soil water content (SWC; $m^3\ m^{-3}$) has been measured using a time domain reflectometry probe (TRIME FM3; Imko, Ettlingen, Germany) every 3 weeks since 2003 in depth profiles of 0.2–2.6 m every 0.2 m, in 10 tubes located along a 1 km transect that crosses the Guyaflux site. At least one tube is located in each of the four terra firme soil units Alt, UhS, SLD and DhS. Measurement error, given by the manufacturer, is 5 vol.% for a 25 vol.% water content and may reach 10 vol.% at very high contents (50 vol.%).

Within a 30 m radius of the Guyaflux tower (Alt soil type), changes in trunk circumference were monitored in 2007 and 2008 in 6 dominant trees (*Dicorynia guianensis* 34.8 cm and 41.1 cm in diameter at breast height, *Oxandra asbeckii* 16.8 cm, *Sloanea sp.* 47.5 cm, *Vouacapoua americana* 27.6 cm, *Goupia glabra* 75.5 cm) using automatic dendrometers (SLS 095; *Penny + Giles*, Christchurch, UK). Data were collected at 30-min intervals using a CRX10 datalogger (Campbell Scientific Inc.).

4.2. Model parameters and calibration

Model parameters were established based on the literature and field data. We performed a preliminary sensitivity analysis to quantify the impact of model parameters and their interaction on the decomposition of the *REW* variance. The methodology given in Wernsdoerfer et al. (2008) was used. We chose to keep in the calibration those parameters that accounted for at least 10% of *REW* variance: the ratio $\rho = Tr/PET$, root density parameters, field capacity and permanent wilting point and the *REW* threshold value defining stressed conditions. Parameters that accounted for less of 10% of the variance were set at the value reported in the literature, Table 2. Canopy cover, c, 99%, was estimated by LIDAR measurements (Vincent et al., 2010). For the proportion of rain diverted to the trunks, p_t and trunk capacity S_t, values of 1.3% and 0.06 mm were used, respectively. These are the values measured by Cuartas et al. (2007) in a tropical forest 80 km from Manaus (Brazil). The mean value of k at the study site was assumed to be 0.88 (Cournac et al., 2002), i.e. a value in the upper range of photosynthetically active radiation extinction coefficients for tropical forests, from 0.7 to 0.9 (Wirth et al., 2001). A S_c of 1.9 mm was estimated with the previous fixed parameters for total 20% interception, the mean intercepted precipitation measured by Roche (1982) 30 km from Paracou in a similar forest stand. Mean *PAI* at Paracou is 6.92 (SD = 1.061), mean *PET* 3.97 mm d^{-1} (SD = 1.15) and mean I_0 measured on the Guyaflux tower 586.8 MJ m^{-2} d^{-1} (SD = 174.91) (Bonal et al., 2008). *PET*, *PAI* and I_0 are assumed to be constant. Using the methodology of Bonal

Please cite this article in press as: Wagner, F., et al., Modeling water availability for trees in tropical forests. Agric. Forest Meteorol. (2011), doi:10.1016/j.agrformet.2011.04.012

Table 2
Fixed parameters of the model.

Parameter	Value	Unit	Origin
c	0.99	%	Vincent et al. (2010)
$\bar{R}$	8.64	mm	Guyaflux data
E_c	0.64	mm	Guyaflux data
p_t	0.013	%	Cuartas et al. (2007)
S_t	0.06	mm	Cuartas et al. (2007)
k	0.88	m^{-1}	Cournac et al. (2002) and Wirth et al. (2001)
threshold	0.4	–	Granier et al. (2007) and Breda et al. (2006)
S_c	1.9	mm	Roche (1982)
I_0	586.8	MJ m^{-2} d^{-1}	Guyaflux data
PAI	6.92	m^2 m^{-2}	Guyaflux data
PET	3.97	mm d^{-1}	Guyaflux data
a	10	%	Granier et al. (1999)

et al. (2008), we assume that a *PAI* of 6.92 is equivalent to a *LAI* above 6, the threshold value above which the ratio between tree transpiration and *PET* is assumed to be constant (Granier et al., 1999).

Two methods are currently used to determine θ_{PWP} and θ_{FC} at the plot scale. The first consists of plotting the water retention curve by collecting field samples and making laboratory measurements using the pressure plate, as by Granier et al. (2007) and Fisher et al. (2008). This approach is expensive and difficult to implement because the structure of the soil sample must be conserved. It is possible to retain the structure in surface samples, but a soil pit is needed to sample a depth profile. Unfortunately, in tropical soils, some horizons are extremely porous, fragile and full of roots, such that conserving the structure of these horizons is impossible. Some surface horizons show very high saturated hydraulic conductivity, with a maximum of $K_s > 500$ mm d^{-1} (Guehl, 1984), making it difficult to saturate the sample. The other problem in this approach is to define the pressure applied to obtain θ_{PWP} and θ_{FC}. The commonly used pressure is −1.5 MPa, but we know that some trees can extract water under −1.5 MPa (Tyree et al., 2003). In addition, this approach is not plant-centered, in other words the significance of values of θ_{PWP} and θ_{FC} are unclear in the absence of roots. The second approach is to use existing pedotransfer functions to plot the water retention curve, as has already been used in Amazonian forests (Tomasella et al., 2000; Markewitz et al., 2010). The use of pedotransfer functions and the measurement of uncertainty associated with this approach has been well described by Brimelow et al. (2010). This approach provides water retention curves at different points of pressure. It suffers from the same problem of defining the pressure applied to obtain θ_{PWP} and θ_{FC}, and of a definition of these particular points driven only by hydrology, not by plant uses. In this paper we describe a new approach used to estimate θ_{PWP} and θ_{FC} for which soil texture and physical laboratory measurements are not needed.

Parameters ρ (*tree transpiration/PET*), root density (λ_{Rfd}), field capacity ($\theta_{FC,l}$) and permanent wilting point ($\theta_{PWP,l}$) were estimated simultaneously. The model was calibrated at three different resolution levels, tube (M1), soil (M2) or forest level (M3), Table 3 and Appendix D, Fig. D.1. Data from 2007 to 2009 where used for model calibration, and data from 2006 were used for its validation. We chose to keep 2007 and 2009 in the calibration because these years were witness to extreme events, a rare event of 180 mm of precipitation in September 2007 during the height of the dry season, and an exceptional dry period in the middle of the 2009 wet season.

Table 3
Number of parameters used in the estimates according to model resolution level.

Parameter vector	Parameters			
Θ_m	ρ	λ_{Rfd}	θ_{PWP}	θ_{FC}
Θ_{M1}, Tube level	1	N_{tube}	$N_{tube} \times N_{layer}$	$N_{tube} \times N_{layer}$
Θ_{M2}, Soil level	1	N_{soil}	$N_{soil} \times N_{layer}$	$N_{soil} \times N_{layer}$
Θ_{M3}, Forest level	1	1	N_{layer}	N_{layer}

We used a Bayesian framework to estimate model parameters as this is well suited to hierarchical models. Here, the value of a parameter is estimated by its posterior distribution. By definition the posterior distribution is proportional to the product of the likelihood of the model and the parameter prior distribution, Eq. (11). The user chooses the prior distribution based on his prior knowledge of the possible values of the parameter.

$$Data = \{Data_1, \ldots, Data_{N_{tube}}\}$$

and

$$Data_j = \{EW^j_{1,1}, \ldots, EW^j_{N_{obs},1}, EW^j_{1,2}, \ldots, EW^j_{1,N_{day}}, \ldots, EW^j_{N_{obs},N_{day}}\} \quad (10)$$

where *Data* corresponds to the values of extractable water measured on number of days of field measurements N_{day}, for the number of TDR probe measurements by tubes N_{obs} and for number of tubes N_{tube}.

$$\pi_m(\Theta_m|Data) \propto \mathcal{L}(Data|\Theta_m)\pi^0_m(\Theta_m) \quad (11)$$

where $m \in \{M1, M2, M3\}$ is the model resolution level, Θ_m the parameter vector values, $\pi_m(\Theta_m \,|\, Data)$ the posterior distribution of the parameters, $\mathcal{L}(Data|\Theta_m)$ model likelihood given the parameter Θ_m and $\pi^0_m(\Theta_m)$ is the prior distribution of the parameters.

We assumed that measurement errors were distributed according to a centered normal distribution with a standard deviation of 20% around the measured value. This standard deviation was chosen to be consistent with the TDR probe error as given by its manufacturer. The error corresponds to the maximum error of the probe for soil water content near 50%, and such high soil water contents never occurred in the TDR probe data. The probe measurement error is multiplicative, increasing with soil water content. The likelihood is then given by:

$$\begin{aligned}\mathcal{L}(Data|\Theta_m) &= \prod_{p=1}^{N_{tube}} \mathcal{L}(Data_p|\Theta_m) \\ &= \prod_{p=1}^{N_{tube}} \prod_{d=1}^{N_{day}} \prod_{l=1}^{N_{layer}} \frac{\exp[-((\widehat{EW^p_{l,d}} - EW^p_{l,d})^2)/(2(0.2 \times EW^p_{l,d})^2)]}{\sqrt{2\pi(0.2 \times EW^p_{l,d})}} \end{aligned} \quad (12)$$

where $\widehat{EW}^p_{l,d}$ are the extractable water values predicted by the model.

The posterior densities of the different parameters were estimated using a Monte Carlo Markov Chain algorithm (Robert and Casella, 2004). As the model contained many parameters, we built a Metropolis-Hastings algorithm within a Gibbs algorithm. Unlike the situation with a Metropolis-Hasting algorithm where the parameters are updated together, in our algorithm each parameter is updated separately and this, when many parameters need to be inferred, increases convergence speed. Details on the algorithm are given in Appendix B.

The same priors for each parameter were used at all three model resolution levels. We used uniform priors as we had no prior knowledge regarding the value of these parameters. To simplify, we give the prior distributions for the forest model, M3.

$$\pi^0_\rho = \mathcal{U}_{[0,1]} \quad (13)$$

$$\pi^0_{\lambda_{Rfd}} = \mathcal{U}_{[0,10]} \quad (14)$$

$$\pi^0_{\theta_{PWP},\theta_{FC};1,\ldots,N_{layer}} = \mathcal{U}_{[0 \le \theta_{PWP;1,\ldots,N_{layer}} < \theta_{FC;1,\ldots,N_{layer}} \le 1]} \quad (15)$$

The algorithm was run for 120,000 iterations. The first 20,000 iterations were discarded as spin-up. Thinning of 100 iterations was

Please cite this article in press as: Wagner, F., et al., Modeling water availability for trees in tropical forests. Agric. Forest Meteorol. (2011), doi:10.1016/j.agrformet.2011.04.012

Table 4
RMSEP for model resolution levels M1, M2 and M3.

Soil	Tube	RMSEP of extractable water, median ± (95% ci)		
		Tube level (M1)	Soil level (M2)	Forest level (M3)
Alt	1	1.696 (1.654–1.756)	2.631 (2.618–2.650)	3.582 (3.576–3.592)
Alt	2	2.032 (1.978–2.108)		
Alt	4	1.819 (1.747–1.903)		
Alt	13	1.897 (1.817–1.992)		
SLD	5	1.943 (1.884–2.022)	3.176 (3.163–3.193)	
SLD	9	1.770 (1.741–1.819)		
SLD	18	2.684 (2.663–2.716)		
DhS	19	4.420 (4.326–4.563)	4.184 (4.126–4.252)	
DhS	7	2.888 (2.815–2.998)		
UhS	16	1.570 (1.512–1.653)	1.570 (1.510–1.658)	

used to remove autocorrelation in the Monte Carlo Markov chains. We used the median of the posterior densities to estimate the parameters, and the distribution of the posterior densities to estimate parameter uncertainties 95% Bayesian credibility intervals (95% ci).

4.3. Quality of fit and validation

The three model resolution levels were compared using the Bayesian information criterion-Monte(Carlo), BICM (Raftery et al., 2007),

$$BICM = 2\hat{\mathcal{L}}_{\max} - N_{par} \times \log(N_{day} \times N_{tdr}) \quad (16)$$

where $\hat{\mathcal{L}}_{\max}$ is the maximum likelihood of the chains, N_{par} is the number of parameters, N_{day} the number of observation days, and N_{tdr} the number of TDR probe measurement. Prediction quality was assessed by computing the root mean square errors of the predictions, RMSEP,

$$RMSEP = \sqrt{\sum_{t=1}^{N_{tube}} \sum_{d=1}^{N_{day}} \sum_{l=1}^{N_{tdr}} \frac{\left(EW^t_{l,d} - \overline{EW^t}_{l,d}\right)^2}{N_{tube} \times N_{day} \times N_{tdr}}} \quad (17)$$

where $\overline{EW^t_{l,d}}$ is the mean of model predictions for the layer measured by the probe (from 10 cm above to 10 cm below the depth of the probe measurement).

We used *EW* values measured from the 1 January 2006 to 30 December 2006 for the validation (data not use in the calibration). The model was run using median values for parameter posterior densities of the parameters of the soil level model. We assigned to each 1 cm layer the median posterior density of the permanent wilting point and the field capacity of the nearest probe measurement point, from 1 to 29 cm depth. Each 1 cm layer was assigned

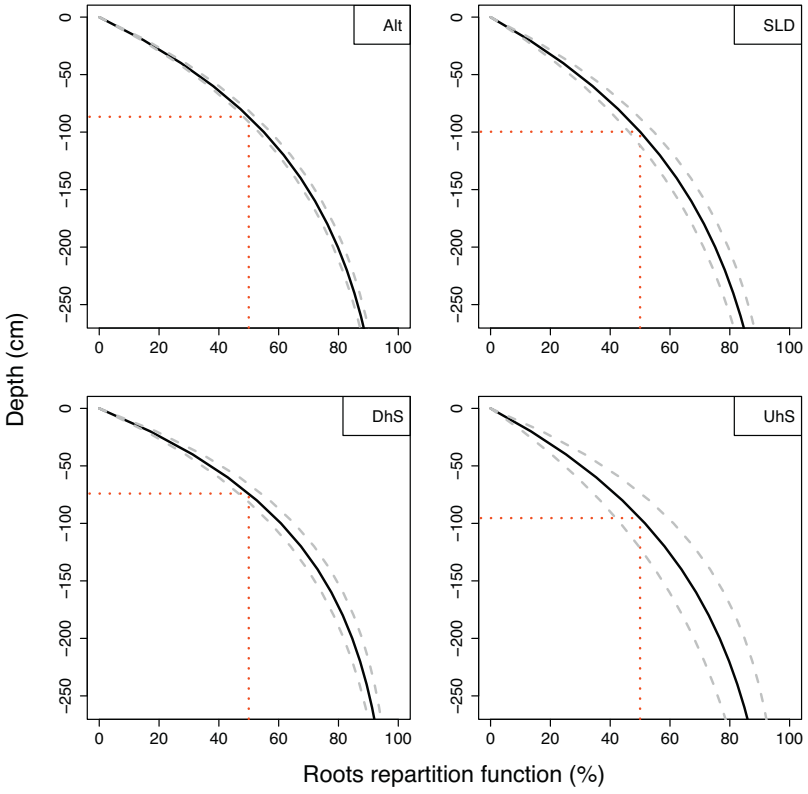

Fig. 2. Roots repartition function obtained for the soil level model M2 (Alt: alloterite at a depth of less than 1.2 m, SLD: superficial lateral drainage, DhS: downhill system, UhS: uphill system). Shown are the 95% Bayesian credibility intervals. Red dotted lines give the soil depths at 50% roots density. (For interpretation of the references to color in this figure legend, the reader is referred to the web version of the article.)

Please cite this article in press as: Wagner, F., et al., Modeling water availability for trees in tropical forests. Agric. Forest Meteorol. (2011), doi:10.1016/j.agrformet.2011.04.012

the permanent wilting point and field capacity given by the 20 cm depth TDR probe measurements, and from 30 to 49 the soil characteristics of the 40 cm depth TDR probe measurements. Predicted values of *EW* and *REW* were compared with measured values.

5. Results

5.1. Model resolution levels

The best resolution selected with the BICM was the forest level, BICM = – 4148.4 (soil level, BICM = – 2066.7; tube level, BICM = – 1250.0). Extractable water RMSEP at all model resolutions ranged from 1.5 to 4.5% of water content, Table 4. With regard to the running soil level in M2, the RMSEP for Alt, SLD, DhS and UhS corresponded to 2.631, 3.176, 4.184 and 1.570 % of water content, respectively.

5.2. Parameters

5.2.1. Ratio ρ, tree transpiration/PET,

At all model resolution levels, i.e. tube (M1), soil (M2) or forest (M3), forest stand transpiration accounted for more than 98% of the *PET*. The median posterior density value of ρ for the forest model was 0.997 (95% ci = 0.986–0.999).

5.2.2. Root fine distribution parameter, λ_{Rfd}

Under non-stressed condition, water was extracted in all the soil layers, with a preference for the water contained in the upper layers, Fig. 2. Indeed, all the posterior values for root density parameter were between 0.005 and 0.01 ($\lambda_{Alt} = 0.0080 \pm (0.0076 - 0.0085)$, $\lambda_{SLD} = 0.0069 \pm (0.0062 - 0.0079)$, $\lambda_{DhS} = 0.0094 \pm (0.0085 - 0.0106)$, $\lambda_{UhS} = 0.0073 \pm (0.0057 - 0.0095)$, $\lambda_{Forest} = 0.0082 \pm (0.0079 - 0.0086)$). The higher the value of λ_{Rfd} the more shallow the rooting. Values for root distribution parameters differed slightly between the soils. Alt, SLD, DhS and UhS soil had respectively 88.4%, 84.6%, 92.0% and 85.9 % of roots between 0 and 270 cm depth. Under non-stressed conditions, in the forest model, 25% of the transpiration was extracted in the horizons above 35 cm, 50% above 85 cm and 75% above 170 cm depth. Differences in root distributions in the forest model and soil model are given in Appendix E, Fig. E.1.

5.2.3. Permanent wilting point, θ_{PWP}

Median θ_{PWP} posterior density values ranged from 3.9 to 17.8% of volumetric water content in M2, Fig. 3. In Alt, SLD and UhS soil, θ_{PWP} slightly increased with depth and the θ_{PWP} profile showed smooth variations. DhS showed sharp θ_{PWP} variations from 80 to 240 cm depth, with high values for 80, 100, 120 and 240 cm in depth, i.e. 16.0, 17.3, 16.4 and 17.8% of volumetric water content, Fig. 3. Credibility intervals for all four soil types were stable above 120 cm and increased below 120 cm depth.

5.2.4. Field capacity, θ_{FC}

Median θ_{FC} posterior density values ranged from 10.4 to 24.4% of volumetric water content in M2, Fig. 3. The lowest values for estimated field capacity θ_{FC} were near 10% and the maximum value near 24% of water content. The estimated values were slightly higher below 1 m in depth. The θ_{FC} profiles correlated with the θ_{PWP} profile except for DhS between 60 and 160 cm. The credibility intervals showed small variations with depth. With the exception of soil DhS at a depth of 260 cm, all 95% credibility intervals were less than 2% of water content under or above the median value.

5.2.5. Extractable water EW

Soil extractable water profiles are given in Appendix F, Fig. F.1. The median *EW* value varied slightly with soil type. Median *EW* values ranged from 1.3% to 15.3% and correspond to extreme val-

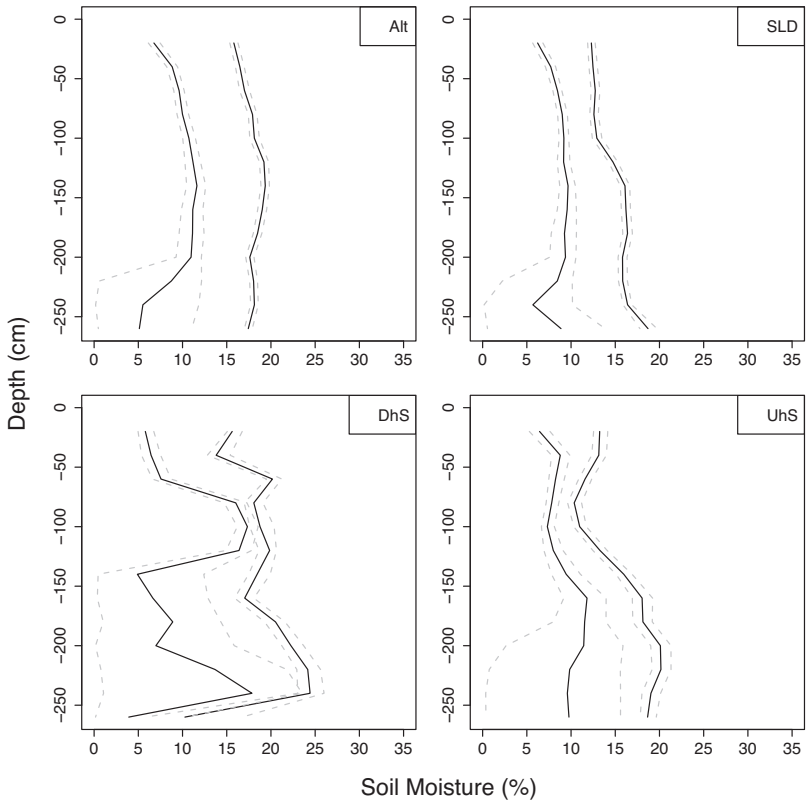

Fig. 3. Permanent wilting points and field capacities obtained for the soil level model M2 (Alt: alloterite at a depth of less than 1.2 m, SLD: superficial lateral drainage, DhS: downhill system, UhS: uphill system). Shown are the 95% Bayesian credibility intervals.

Please cite this article in press as: Wagner, F., et al., Modeling water availability for trees in tropical forests. Agric. Forest Meteorol. (2011), doi:10.1016/j.agrformet.2011.04.012

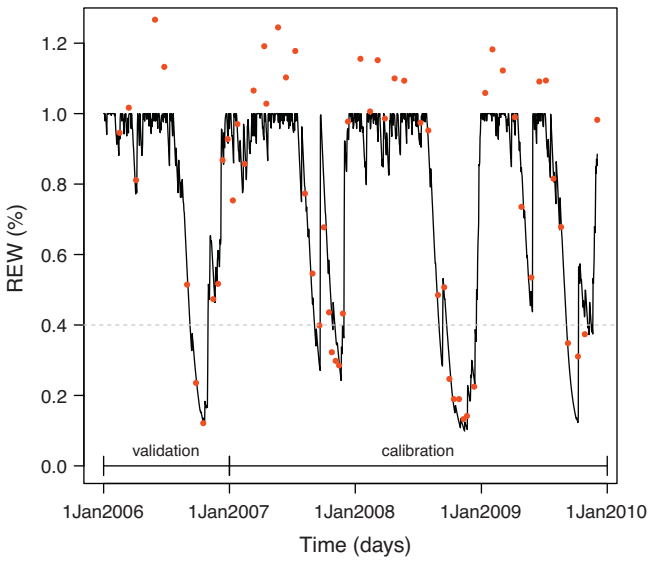

Fig. 4. Seasonal time course of predicted relative extractable water, *REW*, for 2006 (validation) and from 2007 to 2010 (calibration). The points are the observed values of *REW*.

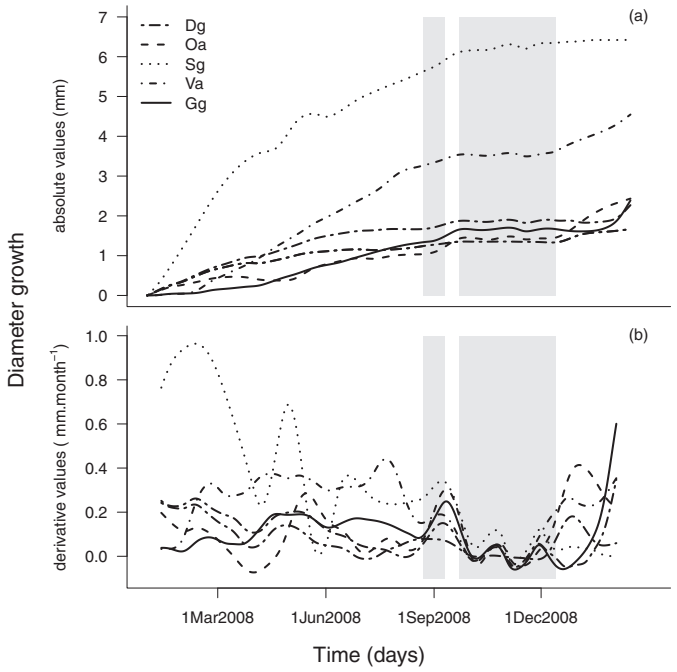

Fig. 5. Diameter growth series (a) and derivatives (b) of *Dicorynia guianensis* (Dg), *Oxandra asbeckii* (Oa), *Sloanea sp* (Sg), *Vouacapoua americana* (Va) and *Goupia glabra* (Gg). Grey font represents *REW* < 0.4

ues for DhS soil. The *EW* profile may be described in three parts. First, a decrease in *EW* is observed in the first 100 cm. Second, from 100 to 200 cm, the *EW* profile and credibility interval remain stable or increase steadily with depth. Under 200 cm, all soils exhibited an increase in *EW* (≥4%) coupled with a marked increase in the credibility interval.

5.3. Model validation

The model was run from 1 January 2006 to 30 December 2006 using the median posterior density values for M2 parameters. Uhs had the smaller RMSEP, 2.24% followed by Alt, SLD and DhS with a RMSEP of 5%, Appendix C, Table C.1. The model successfully reproduced the general trend seen for *REW* variations in 2006 (Fig. 4).

5.4. Variations in relative extractable water, REW

The model reproduced the general trend seen in soil water dynamics from 2006 to 2009, and this for all four soil types, Fig. 4. The model captured the start and end of the dry season. The two unusual events, 180 mm of rain during the dry season in September 2007, and the exceptional drought in the wet season of 2009 were also predicted by the model. In the wet season, the observed *REW* often took a value in excess of 1 whereas maximum *REW* in the model was 1. Agreement was very good between observed and predicted values of *REW*.

5.5. Relative extractable water and stem growth

REW fluctuations matched stem growth measurements in six dominant trees over the period between January 2008 and March 2009, Fig. 5. During the wet season, from January to mid-September, the trees showed different patterns of diameter growth. Four showed a decrease in diameter growth between March and June 2008. When *REW* become critical (≤0.4) between October and December, diameter growth ceased in all the trees.

6. Discussion

In this study we constructed a model of soil water balance for tropical forests and parameterized this model using a dataset collected in Paracou, French Guiana. We then validated this model on an independent dataset from the same forest site. Extractable water is accurately predicted at the three levels of model resolution, i.e. TDR tube, soil type and forest stand, Table 4. At the soil level, RMSEP was always less than 4.2%. This is remarkable considering that precipitation is the only daily step data needed to run the model. Goodness of fit was unaffected by unusual events such as the exceptional rain event in September 2007 during the dry season (c. 180 mm) or the exceptionally dry period during the wet season in 2009, Fig. 4. However, we must acknowledge that the current model does not include porosity (deep drainage through macropores), lateral drainage, run-off, capillarity rise, or potential within-tree root redistribution of water. Our results suggest that these processes are of secondary importance in the accurate prediction of soil water content from our data. Whether they might be needed in other tropical forest sites with different topographic variability, soil properties and rainfall regimes is a worthy question that we intend to test in the near future.

Tree transpiration (*Tr*) accounts for the largest part of ecosystem evapotranspiration (*PET*). At the Paracou forest site, Granier et al. (1996), working in the dry season of 1991, determined the ratio $\rho = Tr/PET$ at 0.75 and observed that this increased up to 0.80–0.85 after a 25 mm rain event. However, other water balance models (e.g. Markewitz et al., 2010) often assume that no soil surface evaporation takes place and that ecosystem evapotranspiration is solely due to tree transpiration. In line with the latter study, we estimated *Tr*/*PET* at 99.7%. This high value may also suggest that we underestimated the water leaving the soil system by lateral and deep drainage. Indeed, some studies report cases where water drains below a given soil layer even though this layer has not reached field capacity (Grimaldi and Boulet, 1989–1990). This process is related to soil porosity, a parameter not taken into account in our model. Including it would greatly increase model complexity as the pores differ in nature and dimensions in the soil layers in our neotropical forest (Grimaldi and Boulet, 1989–1990). Our results nevertheless show that soil porosity is not really needed to accurately simulate soil water content, although its absence prevents us from using the model to simulate *PET*.

Please cite this article in press as: Wagner, F., et al., Modeling water availability for trees in tropical forests. Agric. Forest Meteorol. (2011), doi:10.1016/j.agrformet.2011.04.012

We made the major assumption that soil root density decreases exponentially with depth, and from this we computed the percentage of tree transpiration extracted by the roots from each soil layer. Model predictions suggest that this new approach to modeling root distribution in soil water models is efficient. This manner of modeling root distribution also offers the opportunity to predict the amount of water extracted below the last TDR measurement point, an estimate that is often neglected (Nepstad et al., 2004; Granier et al., 2007). The water extracted at 270 cm ranged from 8 to 15% under non-stressed condition, Fig. 2, consistent with Bonal et al. (2000). However, the water extracted below 250 cm at two other Amazonian sites was estimated to be ca. 30% Markewitz et al. (2010). The difference may be due to differences in root distributions or in soil drainage which is greater at the Tapajós research site over the first 3 m than at Paracou (Guehl, 1984; Belk et al., 2007). We estimated *REW* by explicitly taking account of root density distribution in the soil, Eq. (9), offering the advantage of limiting the weight of the deep layers full of water that contain a negligible proportion of total roots.

Estimated permanent wilting point values are consistent with those obtained for the 0 to 160 cm soil layers in French Guiana by Guehl (1984), ranging from 10 to ca. 15%. As modeled using our DhS soil data, Guehl (1984) registered some profiles of θ_{PWP} exhibiting sharp permanent wilting point variations in less than 40 cm of soil (see Fig. 3). These variations can be explained by a red clay alloterite horizon with very different soil properties (Sabatier et al., 1997). No field measures of field capacities (θ_{FC}) have yet been made of French Guianan soils for comparisons with our estimates (from 3 to 15% of water content). But at two other tropical sites where a long-term tree growth census has been established, Barro Colorado Island (BCI, Panama) and La Selva (Costa Rica), available water capacities reported by Kursar et al. (2005) range respectively from 12 to 29% and 3 to 15% for the upper soil layers (<0.5 m depth). With regard to permanent wilting point, DhS soil showed an uncommon profile. Estimated available water capacity was less than 3% between 80 and 120 cm. This may be explained by a temporarily waterlogged watertable during the rainy season. The presence of this watertable led to no change in the water content of these soil layers, which in turn led to an extremely low extractable water value.

We adapted a Bayesian numerical method to infer model parameters, permanent wilting point θ_{PWP} and field capacity θ_{FC}, using only soil water content values obtained from a TDR probe and a mechanistic model of forest functioning. The first novelty of our approach is that θ_{PWP} and θ_{FC} estimations are entirely data driven. We believe that our approach is more realistic than previous models because we explicitly model water extraction by the forest ecosystem and we do not infer parameter values from soil water content measured at a fixed pressure commonly assumed to be less than −1.5 MPa. Kursar et al. (2009) have shown that drought tolerance differs widely for seedlings of 20 species from central Panama, and Tyree et al. (2003) determined that many woody species tolerate far lower θ_{PWP}. If we consider that each tree species has different and independent sensitivities to θ_{PWP} and θ_{FC}, the values we estimated can be interpreted as averaged θ_{PWP} and θ_{FC} at the forest ecosystem level. Uncertainties in θ_{PWP} and θ_{FC} estimates are explicitly assessed during the calibration procedure using the Bayesian framework we developed. These uncertainties are far more difficult to assess when pedotransfer functions are used, as no standard method is available (Brimelow et al., 2010).

Despite average rainfall of ca. 3000 mm per year, the Paracou site is subject to a 3-month dry season during which rainfall is less than 50 mm per month (Bonal et al., 2008). In 2006 and 2008, *REW* decreased to below 0.2 during this dry season, Fig. 4. In temperate forests, a *REW* value of 0.4 (Granier et al., 2007) has been considered as the limit below which trees experience major physiological stress. In a 1-year growth dataset obtained from the Paracou site we also observed that diameter increments stopped when *REW* < 0.4, Fig. 5. If we apply this threshold, it is evident that the potential period of tree water stress shows marked inter-annual variability, Fig. 4, from 1.5 months in 2007 and 2009 to 3.0 months in 2008. The consequences of this interannual variability on tree functioning, growth and mortality remain to be investigated (but see Fig. 5). Near future measurements of leaf gas exchange and water potential will be used to test whether the 0.4 threshold also characterizes a significant step in leaf gas exchange. Interestingly, we noted a period of drought during the 2009 wet season with exceptionally low rainfall in May (7.2 mm d^{-1} instead of 16.6 mm d^{-1} for the 10-year average), and this led to an exceptional reduction in soil water content.

During wet seasons, an observed *REW* value greater than 1 is relatively frequent (Fig. 4) while the maximum predicted *REW* from our model remains 1 because estimated deep drainage is instantaneous and incoming water exceeding the field capacity is excluded at the daily time step. In other words, soil water content cannot mechanically exceed field capacity in the model. For most soil types during heavy rains, the model therefore does not predict reality. Moreover, lateral drainage events have been observed during heavy rains along hill slopes (Gourlet-Fleury et al., 2004) and so our model may underestimate the water entering the soil along slopes (Daws et al., 2002; Sabatier et al., 1997). Further research should improve these components of the model to take account of wet season conditions in downhill and bottomland systems.

7. Conclusions

In this study we developed, calibrated and validated a daily soil water balance model for use in tropical forests. Precipitation is the only data required with daily precision. The model works with few parameters, most of which are available in the specialized literature. We put forward a novel method to estimate the remaining site-specific parameters, θ_{FC}, θ_{PWP} and λ_{Rfd}, using TDR data only, which should facilitate calibration in other tropical forest sites. The use of a Bayesian framework is a major improvement in the modeling of soil water balance for several reasons. First, it enables us to estimate permanent wilting point (θ_{PWP}), field capacity (θ_{FC}) and their uncertainties by modeling water actually extracted by the roots (not by inferring their values by field measurements). Second, it offers the possibility to infer hierarchical models, e.g. when model parameters are estimated at different levels of integration, such as forest stand/soil types/TDR tubes. The major output of this model is soil *REW*, which may be the most appropriate metric for long-term analyses of tropical forest dynamics under different climatic situations. We believe the model will prove useful in deciphering the relative impact of past environmental and climatic conditions on tree growth and mortality and to explore the expected consequences on tropical forest dynamics of currently simulated future climate scenarios (IPCC, 2007).

Acknowledgements

This manuscript is part of the CLIMFOR project (FRB grant to BH). This study has been possible thanks to the important field work realized at Paracou by B. Burban, J.-Y. Goret, M. Desprez and V. Freycon. We also thank C. Baraloto and two anonymous reviewers who greatly helped improving a previous version of this manuscript.

Appendix A. Soil drainage and characteristics, algorithm details

The model of daily water dynamics may be summed up by the following scheme:

For the top soil layer, if $Th_d \geq 0$:

$$W_{1,d} = Th_d \tag{A.1}$$

where $W_{1,d}$ is the water entering the top layer on day d. Water fills the top layer and extractable water before vegetation uptake ($\widetilde{EW}$) is computed as follows:

$$\text{if} \quad W_{1,d} > EW_1^{\max} - \widehat{EW}_{1,d-1} \begin{cases} W_{2,d} = W_{1,d} - (EW_1^{\max} - \widehat{EW}_{1,d}) \\ \widetilde{EW}_{1,d} = EW_1^{\max} \end{cases} \tag{A.2}$$

$$\text{if} \quad W_{1,d} < EW_1^{\max} - \widehat{EW}_{1,d-1} \begin{cases} W_{2,d} = 0 \\ \widetilde{EW}_{1,d} = \widehat{EW}_{1,d-1} + W_{1,d} \end{cases} \tag{A.3}$$

While $W_{l,d} > 0$ the same process is used to fill the next layers. If any water remains after the last layer (N_{layer}), this is considered to be lost by deep drainage (Dr):

$$\text{if} \quad W_{N_{layer}+1,d} > 0, \quad Dr_d = W_{N_{layer}+1,d} \tag{A.4}$$

Once the water has infiltrated, part of the extractable water is absorbed by trees, and soil plus understorey evapotranspiration.

$$\widehat{EW}_{l,d} = \widetilde{EW}_{l,d} - Tr_{l,d} - Eu_{l,d} \tag{A.5}$$

where $\widehat{EW}_{l,d}$ denotes extractable water, $Tr_{l,d}$ denotes tree transpiration and $Eu_{l,d}$ denotes understorey plus soil evapotranspiration, for layer l on day d.

Appendix B. Metropolis Hastings within Gibbs

Before running the algorithm, the first values of the vector of parameters are initialized.

$$\Theta^0 = \{\theta_1^0, \ldots, \theta_{Npar}^0\} \tag{B.1}$$

where Θ is the vector of parameters θ and $Npar$ the number of parameters.

Then the Metropolis Hastings within Gibbs works in several steps. We give an example for an iteration n and the k th parameters of the vector of parameters.

Generation of a candidate θ_k^* and the new vector of parameters Θ^*:

$$\theta_k^* \sim \pi_\theta^{prop}(\theta_k^{n-1}) \tag{B.2}$$

$$\Theta^* = \{\theta_1^{n-1}, \ldots, \theta_{k-1}^{n-1}, \theta_k^*, \theta_{k+1}^{n-1}, \ldots, \theta_{Npar}^{n-1}\} \tag{B.3}$$

where θ_k^* is a random generation from the proposal distribution π_θ^{prop} which depends on θ_k^{n-1}.

Acceptation or rejection of the new candidate θ_k^* by computing the ratio of the likelihood:

$$\gamma = \underbrace{\frac{\mathcal{L}(Data|\Theta^*)}{\mathcal{L}(Data|\Theta^{n-1})}}_{likelihood} \times \underbrace{\frac{\pi_0(\theta_k^*)}{\pi_0(\theta_k^{n-1})}}_{prior} \times \underbrace{\frac{\pi_\theta^{prop}(\theta_k^{n-1}|\theta_k^*)}{\pi_\theta^{prop}(\theta_k^*|\theta_k^{n-1})}}_{proposal} \wedge 1 \tag{B.4}$$

The candidate θ_k^* is accepted or rejected as follows:

$$u^t \sim \mathcal{U}_{[0,1]}, \quad \theta_k^n \begin{cases} \theta_k^* & if \quad \gamma \geq u^t \\ \theta_k^{n-1} & if \quad \gamma < u^t \end{cases} \tag{B.5}$$

Proposal distribution of the forest level model, M3. The same distribution were use for M1 and M2. Here we give the proposal distribution and boundaries of the distribution.

$$\pi_\rho^{prop} = \mathcal{N}_T(\rho^{t-1}, 0.008); \quad truncated \quad on \quad [0, 100] \tag{B.6}$$

$$\pi_{\lambda_{Rfd}}^{prop} = \mathcal{N}_T(\lambda_{Rfd}^{t-1}, 0.001); [0, 10] \tag{B.7}$$

$$\pi_{\theta_{PWP;l,\ldots,N_{layer}}}^{prop} = \mathcal{N}_T(\theta_{PWP;l,\ldots,N_{layer}}^{t-1}, 0.003); [0, \theta_{FC;l,\ldots,N_{layer}}^{t-1}[\tag{B.8}$$

$$\pi_{\theta_{FC;l,\ldots,N_{layer}}}^{prop} = \mathcal{N}_T(\theta_{FC;l,\ldots,N_{layer}}^{t-1}, 0.003);]\theta_{PWP;l,\ldots,N_{layer}}^{t}, 1] \tag{B.9}$$

Appendix C. Quality of the soil level model's predictions

See Table C.1.

Table C.1
Root Mean Square Error of Prediction (RMSEP) between observed and predicted values of extractable water obtained using the soil level model M2 with the validation dataset (year 2006).

Soil	Tube	RMSEP
Alt	1	2.92
Alt	2	2.97
Alt	4	3.25
Alt	13	3.51
SLD	5	4.11
SLD	9	3.61
SLD	18	3.37
DhS	7	4.00
DhS	19	5.00
UhS	16	2.24

Appendix D. Nested structure of the model

See Fig. D.1.

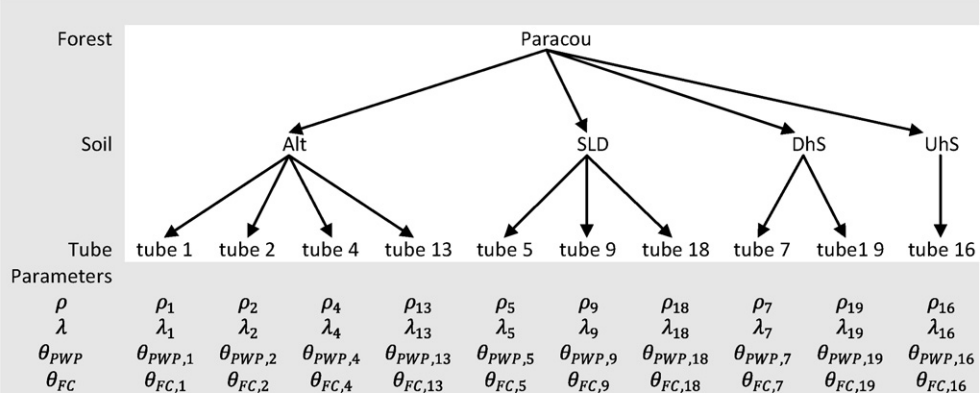

Fig. D.1. Nested structure of the model. M1, tube level: $\rho_1 = \rho_2 = \cdots = \rho_{16}$; M2, soil level: $\rho_1 = \rho_2 = \cdots = \rho 16$, $\lambda_1 = \lambda_2 = \lambda_4 = \lambda_{13}$, $\lambda_5 = \lambda_9 = \lambda_{18}$, $\lambda_7 = \lambda_{19}$, $\theta_{PWP,1} = \theta_{PWP,2} = \theta_{PWP,4} = \theta_{PWP,13}$, $\theta_{PWP,5} = \theta_{PWP,9} = \theta_{PWP,18}$, $\theta_{PWP,7} = \theta_{PWP,19}$, $\theta_{FC,1} = \theta_{FC,2} = \theta_{FC,4} = \theta_{FC,13}$, $\theta_{FC,5} = \theta_{FC,9} = \theta_{PWP,18}$, $\theta_{FC,7} = \theta_{FC,19}$; M3, forest model: $\rho_1 = \rho_2 = \cdots = \rho_{16}$, $\lambda_1 = \lambda_2 = \cdots = \lambda_{16}$, $\theta_{PWP,1} = \theta_{PWP,2} = \cdots = \theta_{PWP,16}$, $\theta_{FC,1} = \theta_{FC,2} = \cdots = \theta_{FC,16}$; Alt: alloterite at a depth of less than 1.2 m, SLD: superficial lateral drainage, DhS: downhill system, UhS: uphill system.

Please cite this article in press as: Wagner, F., et al., Modeling water availability for trees in tropical forests. Agric. Forest Meteorol. (2011), doi:10.1016/j.agrformet.2011.04.012

Appendix E. Difference of roots repartition function

See Fig. E.1.

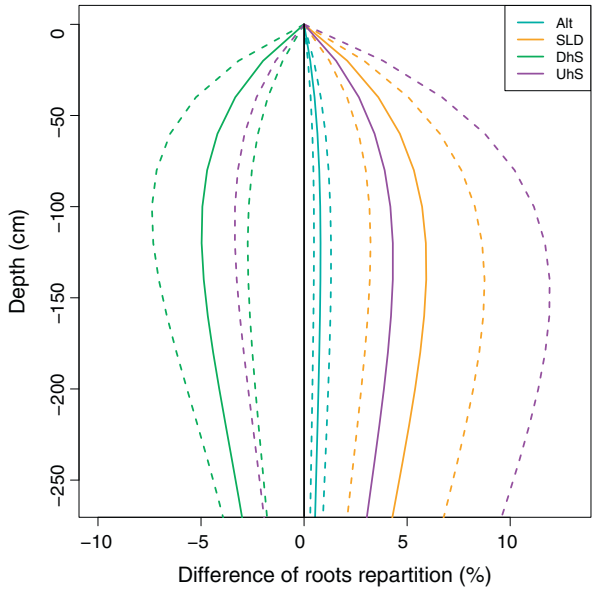

Fig. E.1. Difference of roots repartition function between the forest level model (M3, the plain vertical line) and the soil level model (M2, Alt: alloterite at a depth of less than 1.2 m, SLD: superficial lateral drainage, DhS: downhill system, UhS: uphill system). Shown are the Bayesian 95% credibility intervals.

Appendix F. Examples of extractable water profiles

See Fig. F.1.

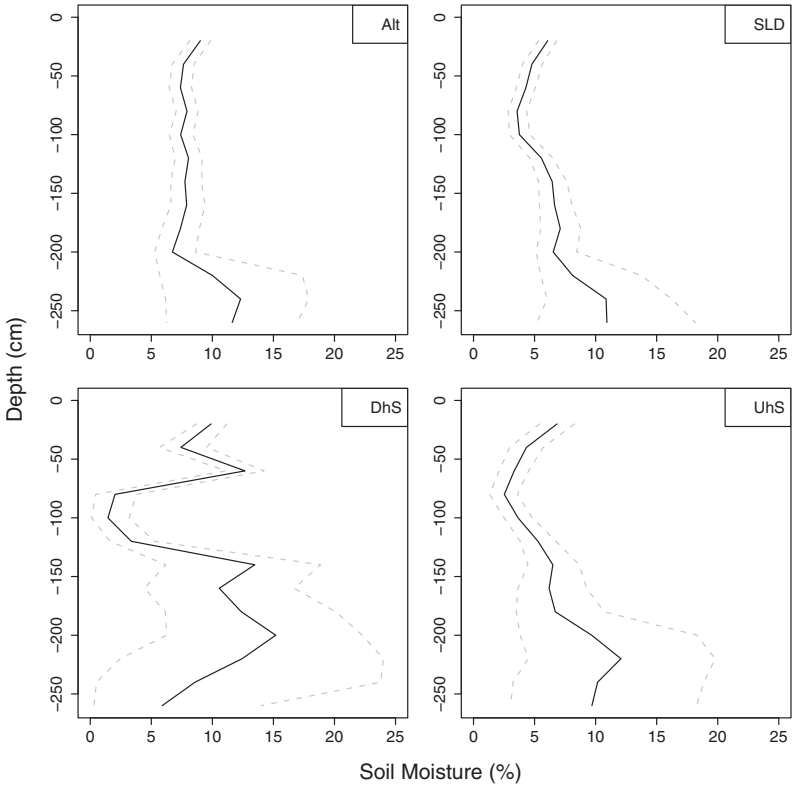

Fig. F.1. Profiles of extractable water obtained for the soil level model M2 (Alt: alloterite at a depth of less than 1.2 m, SLD: superficial lateral drainage, DhS: downhill system, UhS: uphill system). Shown are the 95% Bayesian credibility intervals.

References

Allen, R., Pereira, R., Raes, D., Smith, M., 1998. Crop evapotranspiration – guidelines for computing crop water requirements – Irrigation and Drainage Paper 56. United Nations Food and Agriculture Organization, Rome, Italy.

Belk, E.L., Markewitz, D., Rasmussen, T.C., Maklouf Carvalho, E.J., Nepstad, D.C., Davidson, E.A., 2007. Modeling the effects of throughfall reduction on soil water content in a Brazilian Oxisol under a moist tropical forest. Water Resources Research 43.

Bonal, D., Atger, C., Barigah, T., Ferhi, A., Guehl, J., Ferry, B., 2000. Water acquisition patterns of two wet tropical canopy tree species of French Guiana as inferred from (H_2O)-O-18 extraction profiles. Annals of Forest Science 57, 717–724.

Bonal, D., Bosc, A., Ponton, S., Goret, J.Y., Burban, B., Gross, P., Bonnefond, J.M., Elbers, J., Longdoz, B., Epron, D., Guehl, J.M., Granier, A., 2008. Impact of severe dry season on net ecosystem exchange in the Neotropical rainforest of French Guiana. Global Change Biology 14, 1917–1933.

Boulet, R., Lucas, Y., Fritsch, E., Paquet, H., 1993. Géochimie des paysages: le rôle des couvertures pédologiques. In: Paquet, H., Clauer, H., (Eds.), Sédimentologie et Géochimie de la surface, à la mémoire de Georges Millot, pp. 55–76.

Breda, N., Huc, R., Granier, A., Dreyer, E., 2006. Temperate forest trees and stands under severe drought: a review of ecophysiological responses, adaptation processes and long-term consequences. Annals of Forest Science 63, 625–644.

Brimelow, J.C., Hanesiak, J.M., Raddatz, R., 2010. Validation of soil moisture simulations from the PAMII model, and an assessment of their sensitivity to uncertainties in soil hydraulic parameters. Agricultural and Forest Meteorology 150, 100–114.

Clark, D.A., 2004. Sources or sinks? The responses of tropical forests to current and future climate and atmospheric composition. Philosophical Transactions of the Royal Society of London Series B-Biological Sciences 359, 477–491.

Clark, D.A., 2007. Detecting tropical forests' responses to global climatic and atmospheric change: current challenges and a way forward. Biotropica 39, 4–19.

Clark, D.B., Clark, D.A., Oberbauer, S.F., 2010. Annual wood production in a tropical rain forest in NE Costa Rica linked to climatic variation but not to increasing CO_2. Global Change Biology 16, 747–759.

Cournac, L., Dubois, M., Chave, J., Riera, B., 2002. Fast determination of light availability and leaf area index in tropical forests. Journal of Tropical Ecology 18, 295–302.

Cox, P., Betts, R., Collins, M., Harris, P., Huntingford, C., Jones, C., 2004. Amazonian forest dieback under climate-carbon cycle projections for the 21st century. Theoretical and Applied Climatology 78, 137–156, 2nd Large-Scale Biosphere-Atmosphere Science Conference, Manaus, Brazil, July 07–10, 2002.

Cox, P., Betts, R., Jones, C., Spall, S., Totterdell, I., 2000. Acceleration of global warming due to carbon-cycle feedbacks in a coupled climate model. Nature 408, 184–187.

Please cite this article in press as: Wagner, F., et al., Modeling water availability for trees in tropical forests. Agric. Forest Meteorol. (2011), doi:10.1016/j.agrformet.2011.04.012

Cuartas, L.A., Tomasella, J., Nobre, A.D., Hodnett, M.G., Waterloo, M.J., Munera, J.C., 2007. Interception water-partitioning dynamics for a pristine rainforest in Central Amazonia: marked differences between normal and dry years. Agricultural and Forest Meteorology 145, 69–83.

Daws, M., Mullins, C., Burslem, D., Paton, S., Dalling, J., 2002. Topographic position affects the water regime in a semideciduous tropical forest in Panama. Plant and Soil 238, 79–90.

Ferment, A., Picard, N., Gourlet-Fleury, S., Baraloto, C., 2001. A comparison of five indirect methods for characterizing the light environment in a tropical forest. Annals of Forest Science 58, 877–891.

Ferry, B., Morneau, F., Bontemps, J.D., Blanc, L., Freycon, V., 2010. Higher treefall rates on slopes and waterlogged soils result in lower stand biomass and productivity in a tropical rain forest. Journal of Ecology 98, 106–116.

Fisher, R., Williams, M., Do Vale, R., Da Costa, A., Meir, P., 2006. Evidence from Amazonian forests is consistent with isohydric control of leaf water potential. Plant Cell and Environment 29, 151–165.

Fisher, R.A., Williams, M., Da Costa, A.L., Malhi, Y., Da Costa, R.F., Almeida, S., Meir, P., 2007. The response of an Eastern Amazonian rain forest to drought stress: results and modelling analyses from a throughfall exclusion experiment. Global Change Biology 13, 2361–2378.

Fisher, R.A., Williams, M., Ruivo, M.d.L., de Costa, A.L., Meira, P., 2008. Evaluating climatic and soil water controls on evapotranspiration at two Amazonian rainforest sites. Agricultural and Forest Meteorology 148, 850–861.

Gash, J., 1979. Analytical model of rainfall interception by forests. Quarterly Journal of the Royal Meteorological Society 105, 43–55.

Gash, J., Lloyd, C., Lachaud, G., 1995. Estimating sparse forest rainfall interception with an analytical model. Journal of Hydrology 170, 79–86.

Germer, S., Elsenbeer, H., Moraes, J.M., 2006. Throughfall and temporal trends of rainfall redistribution in an open tropical rainforest, south-western Amazonia (Rondonia, Brazil). Hydrology and Earth System Sciences 10, 383–393.

Goulden, M., Miller, S., da Rocha, H., Menton, M., de Freitas, H., Figueira, A., de Sousa, C., 2004. Diel and seasonal patterns of tropical forest CO_2 exchange. Ecological Applications 14, S42–S54.

Gourlet-Fleury, S., Guehl, J.M., Laroussinie, O., 2004. Ecology and management of a neotropical rainforest – lessons drawn from Paracou, a long-term experimental research site in French Guiana. Elsevier.

Graham, E.A., Mulkey, S.S., Kitajima, K., Phillips, N.G., Wright, S.J., 2003. Cloud cover limits net CO_2 uptake and growth of a rainforest tree during tropical rainy seasons. Proceedings of the National Academy of Sciences of the United States of America 100, 572–576.

Granier, A., Breda, N., Biron, P., Villette, S., 1999. A lumped water balance model to evaluate duration and intensity of drought constraints in forest stands. Ecological Modelling 116, 269–283.

Granier, A., Huc, R., Barigah, S., 1996. Transpiration of natural rain forest and its dependence on climatic factors. Agricultural and Forest Meteorology 78, 19–29.

Granier, A., Reichstein, M., Breda, N., Janssens, I.A., Falge, E., Ciais, P., Gruenwald, T., Aubinet, M., Berbigier, P., Bernhofer, C., Buchmann, N., Facini, O., Grassi, G., Heinesch, B., Ilvesniemi, H., Keronen, P., Knohl, A., Koestner, B., Lagergren, F., Lindroth, A., Longdoz, B., Loustau, D., Mateus, J., Montagnani, L., Nys, C., Moors, E., Papale, D., Peiffer, M., Pilegaard, K., Pita, G., Pumpanen, J., Rambal, S., Rebmann, C., Rodrigues, A., Seufert, G., Tenhunen, J., Vesala, I., Wang, Q., 2007. Evidence for soil water control on carbon and water dynamics in European forests during the extremely dry year: 2003. Agricultural and Forest Meteorology 143, 123–145.

Grimaldi, M., Boulet, R., 1989–1990. Relation entre l'espace poral et le fonctionnement hydrodynamique d'une couverture pédologique sur socle de guyane française. Cahier de l'ORSTOM, série Pédologie XXV, pp. 263–275.

Guehl, J.M., 1984. Dynamique de l'eau dans le sol en forêt tropicale humide guyanaise. Influence de la couverture pédologique. Annals of Forest Science 41, 195–236.

Humbel, F.X., 1978. Caractérisation, par des mesures physiques, hydriques et d'enracinement, de sols de Guyane française à dynamique de l'eau superficielle. Sciences du Sol 2, 83–94.

Hutyra, L.R., Munger, J.W., Saleska, S.R., Gottlieb, E., Daube, B.C., Dunn, A.L., Amaral, D.F., de Camargo, P.B., Wofsy, S.C., 2007. Seasonal controls on the exchange of carbon and water in an Amazonian rain forest. Journal of Geophysical Research – Biogeosciences 112.

IPCC, 2007. Climate Change 2007. The Fourth Assessment Report (AR4).

Kursar, T., Engelbrecht, B., Tyree, M., 2005. A comparison of methods for determining soil water availability in two sites in Panama with similar rainfall but distinct tree communities. Journal of Tropical Ecology 21, 297–305.

Kursar, T.A., Engelbrecht, B.M.J., Burke, A., Tyree, M.T., El Omari, B., Giraldo, J.P., 2009. Tolerance to low leaf water status of tropical tree seedlings is related to drought performance and distribution. Functional Ecology 23, 93–102.

Lloyd, C., Gash, J., Shuttleworth, W., 1988. The measurement and modelling of rainfall interception by Amazonian rain forest. Agricultural and Forest Meteorology 43, 277–294.

Malhi, Y., Aragao, L.E.O.C., Galbraith, D., Huntingford, C., Fisher, R., Zelazowski, P., Sitch, S., McSweeney, C., Meir, P., 2009. Exploring the likelihood and mechanism of a climate-change-induced dieback of the Amazon rainforest. Proceedings of the National Academy of Sciences of the United States of America 106, 20610–20615.

Malhi, Y., Wright, J., 2004. Spatial patterns and recent trends in the climate of tropical rainforest regions. Philosophical Transactions of the Royal Society of London Series B-Biological Sciences 359, 311–329.

Marengo, J., 1992. Interannual variability of surface climate in the Amazon basin. International Journal of Climatology 12, 853–863.

Markewitz, D., Devine, S., Davidson, E.A., Brando, P., Nepstad, D.C., 2010. Soil moisture depletion under simulated drought in the Amazon: impacts on deep root uptake. New Phytologist 187, 592–607.

Miranda, E., Vourlitis, G., Priante, N., Priante, P., Campelo, J., Suli, G., Fritzen, C., Lobo, F., Shiraiwa, S., 2005. Seasonal variation in the leaf gas exchange of tropical forest trees in the rain forest-savanna transition of the southern Amazon Basin. Journal of Tropical Ecology 21, 451–460.

Muzylo, A., Llorens, P., Valente, F., Keizer, J.J., Domingo, F., Gash, J.H.C., 2009. A review of rainfall interception modelling. Journal of Hydrology 370, 191–206.

Nepstad, D., Lefebvre, P., Da Silva, U.L., Tomasella, J., Schlesinger, P., Solorzano, L., Moutinho, P., Ray, D., Benito, J.G., 2004. Amazon drought and its implications for forest flammability and tree growth: a basin-wide analysis. Global Change Biology 10, 704–717.

Nepstad, D.C., Tohver, I.M., Ray, D., Moutinho, P., Cardinot, G., 2007. Mortality of large trees and lianas following experimental drought in an Amazon forest. Ecology 88, 2259–2269.

Phillips, O.L., Aragao, L.E.O.C., Lewis, S.L., Fisher, J.B., Lloyd, J., Lopez-Gonzalez, G., Malhi, Y., Monteagudo, A., Peacock, J., Quesada, C.A., van der Heijden, G., Almeida, S., Amaral, I., Arroyo, L., Aymard, G., Baker, T.R., Banki, O., Blanc, L., Bonal, D., Brando, P., Chave, J., Alves de Oliveira, A.C., Cardozo, N.D., Czimczik, C.I., Feldpausch, T.R., Freitas, M.A., Gloor, E., Higuchi, N., Jimenez, E., Lloyd, G., Meir, P., Mendoza, C., Morel, A., Neill, D.A., Nepstad, D., Patino, S., Cristina Penuela, M., Prieto, A., Ramirez, F., Schwarz, M., Silva, J., Silveira, M., Thomas, A.S., ter Steege, H., Stropp, J., Vasquez, R., Zelazowski, P., Alvarez Davila, E., Andelman, S., Andrade, A., Chao, K.J., Erwin, T., Di Fiore, A., Honorio, C.E., Keeling, H., Killeen, T.J., Laurance, W.F., Pena Cruz, A., Pitman, N.C.A., Nunez Vargas, P., Ramirez-Angulo, H., Rudas, A., Salamao, R., Silva, N., Terborgh, J., Torres-Lezama, A., 2009. Drought Sensitivity of the Amazon Rainforest. Science 323, 1344–1347.

Phillips, O.L., van der Heijden, G., Lewis, S.L., Lopez-Gonzalez, G., Aragao, L.E.O.C., Lloyd, J., Malhi, Y., Monteagudo, A., Almeida, S., Alvarez Davila, E., Amaral, I., Andelman, S., Andrade, A., Arroyo, L., Aymard, G., Baker, T.R., Blanc, L., Bonal, D., Alves de Oliveira, A.C., Chao, K.J., Davila Cardozo, N., da Costa, L., Feldpausch, T.R., Fisher, J.B., Fyllas, N.M., Freitas, M.A., Galbraith, D., Gloor, E., Higuchi, N., Honorio, E., Jimenez, E., Keeling, H., Killeen, T.J., Lovett, J.C., Meir, P., Mendoza, C., Morel, A., Nunez Vargas, P., Patino, S., Peh, K.S.H., Pena Cruz, A., Prieto, A., Quesada, C.A., Ramirez, F., Ramirez, H., Rudas, A., Salamao, R., Schwarz, M., Silva, J., Silveira, M., Slik, J.W.F., Sonke, B., Thomas, A.S., Stropp, J., Taplin, J.R.D., Vasquez, R., Vilanova, E., 2010. Drought-mortality relationships for tropical forests. New Phytologist 187, 631–646.

Raftery, A.E., Newton, M.A., Satagopan, J.M., Krivitsky, P.N., 2007. Bayesian statistics. Oxford University Press. Chapter Estimating the Integrated Likelihood via Posterior Simulation Using the Harmonic Mean Identity, pp. 1–45.

Robert, C.P., Casella, G., 2004. Monte Carlo Statistical Methods. Springer texts in statistics, 2nd ed. Springer.

Roche, M.A., 1982. Evapotranspiration réelle de la forêt amazonienne en Guyane. Cahiers ORSTOM, Sèrie Hydrologie 19, 37–44.

Rutter, A., Kershaw, K., Robins, P., Morton, A., 1971. A predictive model of rainfall interception in forests. i. Derivation of the model from observations in a plantation of Corsican pine. Agricultural Meteorology 9, 367–384.

Sabatier, D., Grimaldi, M., Prevost, M., Guillaume, J., Godron, M., Dosso, M., Curmi, P., 1997. The influence of soil cover organization on the floristic and structural heterogeneity of a Guianan rain forest. Plant Ecology 131, 81–108.

Sombroek, W., 2001. Spatial and temporal patterns of Amazon rainfall – consequences for the planning of agricultural occupation and the protection of primary forests. Ambio 30, 388–396.

ter Steege, H., Pitman, N.C.A., Phillips, O.L., Chave, J., Sabatier, D., Duque, A., Molino, J.F., Prevost, M.F., Spichiger, R., Castellanos, H., von Hildebrand, P., Vasquez, R., 2006. Continental-scale patterns of canopy tree composition and function across Amazonia. Nature 443, 444–447.

Tomasella, J., Hodnett, M., Rossato, L., 2000. Pedotransfer functions for the estimation of soil water retention in Brazilian soils. Soil Science Society of America Journal 64, 327–338.

Tyree, M., Engelbrecht, B., Vargas, G., Kursar, T., 2003. Desiccation tolerance of five tropical seedlings in Panama. Relationship to a field assessment of drought performance. Plant Physiology 132, 1439–1447.

Valente, F., David, J., Gash, J., 1997. Modelling interception loss for two sparse eucalypt and pine forests in central Portugal using reformulated Rutter and Gash analytical models. Journal of Hydrology 190, 141–162.

Vincent, G., Weissenbacher, E., D., S., Blanc, L., Proisy, C., Couteron, P., 2010. Détection des variations de structure de peuplements en forêt dense tropicale humide par Lidar aéroporté (Small foot-print airborn LiDAR proves highly sensitive to changes in structure of moist tropical forest). Revue Française de Photogrammétrie et Télédectection 191, 42–50.

Wagner, F., Rutishauser, E., Blanc, L., Herault, B., 2010. Effects of plot size and census interval on descriptors of forest structure and dynamics. Biotropica 42, 664–671.

Wernsdoerfer, H., Rossi, V., Cornu, G., Oddou-Muratorio, S., Gourlet-Fleury, S., 2008. Impact of uncertainty in tree mortality on the predictions of a tropical forest dynamics model. Ecological Modelling 218, 290–306.

Wirth, R., Weber, B., Ryel, R., 2001. Spatial and temporal variability of canopy structure in a tropical moist forest. Acta Oecologica-International Journal of Ecology 22, 235–244.

Xiao, X., Hagen, S., Zhang, Q., Keller, M., Moore III, B., 2006. Detecting leaf phenology of seasonally moist tropical forests in South America with multi-temporal MODIS images. Remote Sensing of Environment 103, 465–473.

Please cite this article in press as: Wagner, F., et al., Modeling water availability for trees in tropical forests. Agric. Forest Meteorol. (2011), doi:10.1016/j.agrformet.2011.04.012